frontiers in Chemical Engineering

ORIGINAL RESEARCH
published: 29 March 2022
doi: 10.3389/fceng.2022.748549

Controllable Degradable Plasma Electrolytic Oxidation Coated Mg Alloy for Biomedical Application

Xiaopeng Lu[1]*, *Carsten Blawert*[2], *Bérengère J.C. Luthringer*[2] and *Mikhail L. Zheludkevich*[2,3]

[1]Shenyang National Laboratory for Materials Science, Northeastern University, Shenyang, China, [2]Helmholtz-Zentrum Hereon, Institute of Surface Science, Geesthacht, Germany, [3]Faculty of Engineering, University of Kiel, Kiel, Germany

A controllable degradable coating on Mg alloy based on plasma electrolytic oxidation (PEO) process is reported for the first time. The reported results show that introduction of silica nanoparticles into PEO electrolytes leads to their reactive incorporation in coatings and thus influencing the degradation behavior. Dissolution of amorphous phases facilitates chemical reaction with components of simulated body fluid, resulting in self-healing effect *via* redeposition of insoluble conversion products. The dynamic balance between dissolution of the original coating and reconstruction of corrosion layer is mainly determined by the phase composition of the coating as well as the surrounding corrosive medium.

Keywords: magnesium, plasma electrolytic oxidation, biodegrability, nanoparticle, degradation

OPEN ACCESS

Edited by:
Aditya Kumar,
Indian Institute of Technology Dhanbad, India

Reviewed by:
Apurba Sinhamahapatra,
Indian Institute of Technology Dhanbad, India
Priya Varshney,
National Institute of Technology Rourkela, India

***Correspondence:**
Xiaopeng Lu
luxiaopeng@mail.neu.edu.cn

Specialty section:
This article was submitted to Surface and Interface Engineering, a section of the journal Frontiers in Chemical Engineering

Received: *28 July 2021*
Accepted: *11 March 2022*
Published: *29 March 2022*

Citation:
Lu X, Blawert C, Luthringer BJC and Zheludkevich ML (2022) Controllable Degradable Plasma Electrolytic Oxidation Coated Mg Alloy for Biomedical Application. Front. Chem. Eng. 4:748549. doi: 10.3389/fceng.2022.748549

1 INTRODUCTION

Magnesium and its alloys are of great interest for biomedical applications (Hort et al., 2010; Cha et al., 2013). However, the uncontrollable corrosion or degradation rate is the main obstacle for Mg to be used as biodegradable implant material (Staiger et al., 2006; Miskovic et al., 2017; Song et al., 2020). Alloying and surface treatment are the main approaches to tailor the corrosion rate of magnesium-based biomaterials (Tie et al., 2021; Yang et al., 2021). It was found that some potential alloying elements raise certain alarms concerning toxicity and biocompatibility. Furthermore, it is also out of the question to control the degradation rate of Mg only by introduction of alloying elements (Wu et al., 2013; Sankara Narayanan et al., 2014). Therefore, a variety of surface treatment processes have been utilized to better protect Mg from corrosive attack (Song et al., 2007; Córdoba et al., 2016; Gnedenkov et al., 2016; Ke et al., 2016). Nevertheless, not all of them can be used for biomedical applications since certain coatings are designed for corrosion protection rather than controlling the degradation rate of Mg substrate. In general, coating material for biodegradable implants should meet several important requirements. The key properties are biocompatibility, controllable degradation rate, good adhesion to the substrate, and acceptable wear resistance. Among which, control of the initial degradation is of paramount importance (Kirkland et al., 2010). Although polymer coatings have been applied to control the degradation rate of metallic material, the main drawback is the poor adhesion to the metal surface when corrosion occurs (Hu et al., 2012). An attractive alternative is coating formed by plasma electrolytic oxidation (PEO) which is an environmentally friendly process to produce ceramic-like layers with certain barrier properties and high resistance against wear. These coatings have exhibited good biocompatibility and adhesion ability to the substrate (Blawert et al., 2015; Lu et al., 2015; Sun et al., 2016). The degradation behavior of PEO coating has been proved to be related to the microstructure and phase composition of the oxide layer. The extent of corrosion resistance is mainly dependent on internal coating structure,

with the two key factors, namely the interconnected open porosity and the barrier layer (Arrabal et al., 2009; Zhang et al., 2015). Coatings composed of phases with high chemical stability normally demonstrate better corrosion performance (Mori et al., 2014). Besides the corrosive medium also plays an important role in the degradation process of PEO coatings, which should be taken into consideration if the coatings are used for specific applications, especially in the area of biomedical application. Recently the important activities on the degradation behavior of PEO coating on Mg alloys in simulated body fluid have been started (Zhang et al., 2017; Mei et al., 2020; Mei et al., 2021). Nevertheless, the difficulty in achieving an acceptable control over the degradation rate is still a matter of concern in fabricating PEO coating with a programmed lifetime. Most standard industrial PEO coatings are designed to be insoluble for permanent use and cannot be directly used for Mg implants. Therefore, finding a way of tuning the degradation rate of PEO coatings can lead to a breakthrough in application of Mg-based biodegradable implants.

2 MATERIALS AND METHODS

AM50 magnesium alloy in size of 15 mm × 15 mm × 4 mm was treated by a pulsed DC power supply with a constant current density of 37 mA/cm^2 for 20 min. The duty ratio was 10% and frequency was 250 Hz. During the PEO process, the specimen and stainless-steel tube were used as the anode and cathode, respectively. The chemical composition of AM50 alloy, as measured with an Arc/Spark Optical Emission Spectroscopy system (Spark analyser M9, Spectro Ametek, Germany), is 4.74 wt.% Al, 0.383 wt.% Mn, 0.065 wt.% Zn, 0.063 wt.% Si, 0.002 wt.% Fe, 0.002 wt.% Cu and Mg balance. The specimens were ground using emery sheets up to 2,500 grit and then air-dried prior to PEO treatment. As the voltage was limited at 420 V, the coatings were finally produced under a constant voltage mode after reaching the voltage limitation. 2 and 5 g/L SiO_2 nanoparticles with size of 12 nm avg. were added into phosphate based electrolyte (8 g/L KOH and 20 g/L Na_3PO_4). A stirrer and bubbling generator were used to facilitate the uniform distribution of the particles in the electrolyte. PEO coating without particle addition was produced for comparison. The corresponding coatings are named PPEO, PPEO (2 g_particle) and PPEO (5 g_particle), respectively. The temperature of the electrolytes was kept at 10 ± 2°C by a water-cooling system. A scanning electron microscope (TESCAN Vega3 SB) equipped with EDS was used to examine the microstructure and composition of the PEO coatings. X-ray diffraction (XRD) investigations were carried out using a Siemens diffractometer operating at 40 kV and 40 mA with Cu Kα radiation.

The degradation behavior of the PEO coatings was assessed with electrochemical impedance spectroscopy (EIS) test with an ACM Gill AC computer controlled potentiostat at room temperature. A typical three-electrode cell with the coated specimen as the working electrode, a saturated Ag/AgCl electrode as the reference electrode, and a platinum mesh as counter electrode was used. Electrochemical impedance spectroscopy (EIS) studies were performed at open circuit potential with AC amplitude of 10 mV RMS sinusoidal perturbations over the frequency range from 30 kHz to 0.01 Hz for 7 days, and further immersed up to 1 month for specific samples. Hank's solution (8.00 g NaCl, 0.40 g KCl, 0.14 g $CaCl_2$, 0.35 g $NaHCO_3$, 0.20 g $MgSO_4{\cdot}7H_2O$, 0.12 g $Na_2HPO_4{\cdot}12H_2O$, 0.06 g KH_2PO_4) was prepared according to ASTM-G31-72 (Shi et al., 2009; Gu et al., 2011).

The isolation of primary human osteoblasts was performed according to the Declaration of Helsinki. Human hip joints were obtained from consenting patients undergoing hip arthroplasty (Schön Klinik Hamburg Eilbek, Hamburg, Germany) with the approval of the local ethic committee. Cancellous bone pieces were removed from the hip joint bone and transferred to a cell culture covered with DMEM Glutamax-I (Life Sciences, Karlsruhe, Germany) with 10% fetal bovine serum (FBS, PAA Laboratories GmbH, Linz,

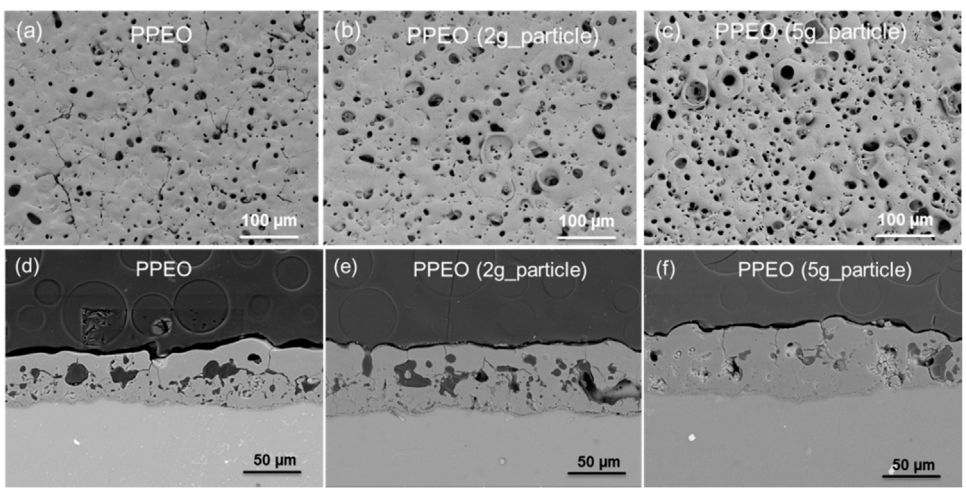

FIGURE 1 | Surface and cross section morphology of the coatings. **(A)** and **(D)** PPEO, **(B)** and **(E)** PPEO (2 g_particle), **(C)** and **(F)** PPEO (5 g_particle).

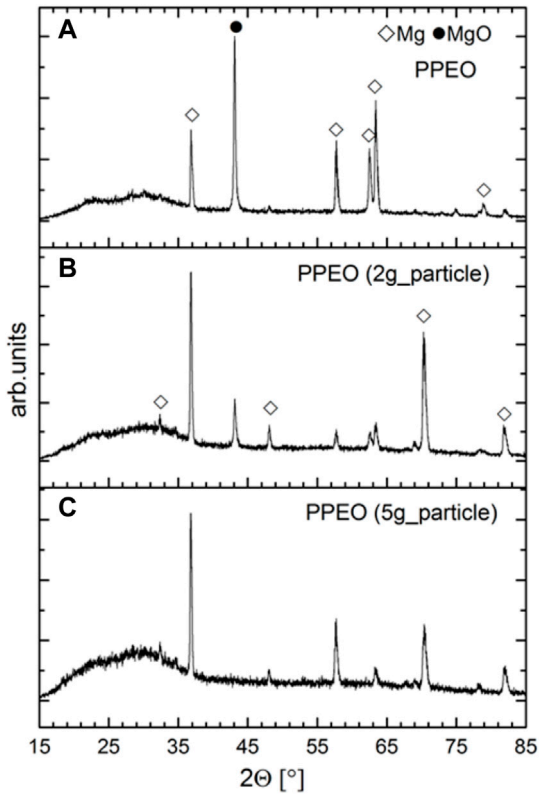

FIGURE 2 | XRD patterns of the PEO coatings. **(A)** PPEO, **(B)** PPEO (2 g_particle), and **(C)** PPEO (5 g_particle).

Austria), and cultured under physiological conditions (5% CO_2, 20% O_2, 95% relative humidity, 37°C) until cell outgrowth. Then, bone pieces were removed and the cells were further cultured until reaching sub-confluent state. For this study osteoblasts were used up to the third passage. 100,000 osteoblasts were seeded on each sample beforehand sterilized with 70% ethanol and cultured for up to 7 days with media exchange every 2–3 days.

For the assessment of osteoblast cell viability and material coverage, the live/dead staining assay (Life Technologies, Darmstadt, Germany) was performed. The staining solution was prepared by adding 4 µl Calcein AM (green stain for viable cells) and 10 µl Ethidium homodimer-1 (red: dead cells) to 10 ml of sterile distilled water. The samples were washed with sterile distilled water to eliminate the non-adherent cells and then immersed in 1.5 ml of staining solution for 20 min under physiological conditions prior to fluorescent microscopy evaluation (Eclipse Ti–S; Nikon, Düsseldorf, Germany). Samples were then critical-point-dried before (SEM) evaluation (Phenom ProX; LOT-Quantum Design GmbH, Darmstadt, Germany). After a glutaraldehyde fixation step, carriers were stained in osmium tetroxide prior to an alcoholic dehydration row. Subsequently, samples were critical-point-dried in 2-propanol to preserve cell morphology by a Leica EM CPD300 (Leica Mikrosysteme Vertrieb GmbH, Wetzlar, Germany).

TABLE 1 | Surface composition (at. %) of the coatings before and after corrosion test.

Coating	O	Na	Mg	Al	Si	P	Ca
PPEO	55	5	28	1	—	11	—
PPEO (2 g_particle)	58	5	24	1	4	9	—
PPEO (5 g_particle)	52	5	22	1	10	9	—
PPEO_corroded	50	3	34	2	—	10	0.5
PPEO (2 g_particle)_corroded	54	2	23	2	5	9	5
PPEO (5 g_particle)_corroded	55	4	15	3.5	12	7	2.5

3 RESULTS AND DISCUSSION

A new particle-containing electrolyte formulation is used for fabricating PEO coating, aiming at designing an amorphous layer and controlling the coating degradation rate. Phase composition of the coating can be changed from crystalline to amorphous by addition of SiO_2 nanoparticles under certain treatment parameters (Lu et al., 2015). The backscattered electron (BSE) micrographs of the surface and cross section of the coatings demonstrate the morphology of the coatings obtained in electrolytes with addition of different concentrations of nanoparticles (**Figure 1**). The layer with higher load seems to be more porous than the other two kinds of coatings. As can be seen from the cross section, the coating is slightly thicker in the presence of particles (63 ± 5 µm) when compared to the blank one (50 ± 5 µm), while the number of particles in the electrolyte has nearly no influence on the thickness of the coating. All PEO coatings consist of an outer relatively compact region divided by a central pore band layer, and an inner thin barrier layer which is hardly visible at the present micrographs.

All the produced coatings contain amorphous phase, as indicated by the large broad bump distributed over 20°–35° in the X-ray diffraction pattern (**Figure 2**). The Mg peaks originate from the substrate. Nevertheless, an important difference in phase composition can be observed. The coating in the absence of nanoparticles consists of crystalline MgO phase, while the layer tends to be fully amorphous with the incorporation of SiO_2 nanoparticles. The intensity of MgO peak decreases to some extent with the addition of 2 g/L particles and then disappears when the particle concentration further increases to 5 g/L. A reactive incorporation between MgO, phosphate and SiO_2 particles is suggested resulting in a new amorphous phase. The chemical composition of different coatings determined by EDS is given in **Table 1**. The content of oxygen and phosphorus is similar for all coatings. As expected, the silicon content in the coating is related to the particle concentration in the electrolyte, since electrolyte with higher concentration of particles leads to higher Si amount in the coating, e.g., 10 at. % for PPEO (5 g_particle) and 4 at. % for PPEO (2 g_particle), respectively. With the identification of P and Na in the coatings, it can be inferred that the amorphous material is composed of mixed oxides of $Na_2O{\cdot}MgO{\cdot}SiO_2$, while glassy solidification is supported by the presence of phosphorus.

A key feature is that the coatings also demonstrate significant difference in the degradation behavior. The surface and cross section of the corroded specimens can be observed in **Figure 3**. The coating surface is dominated by pores and cracks, and the

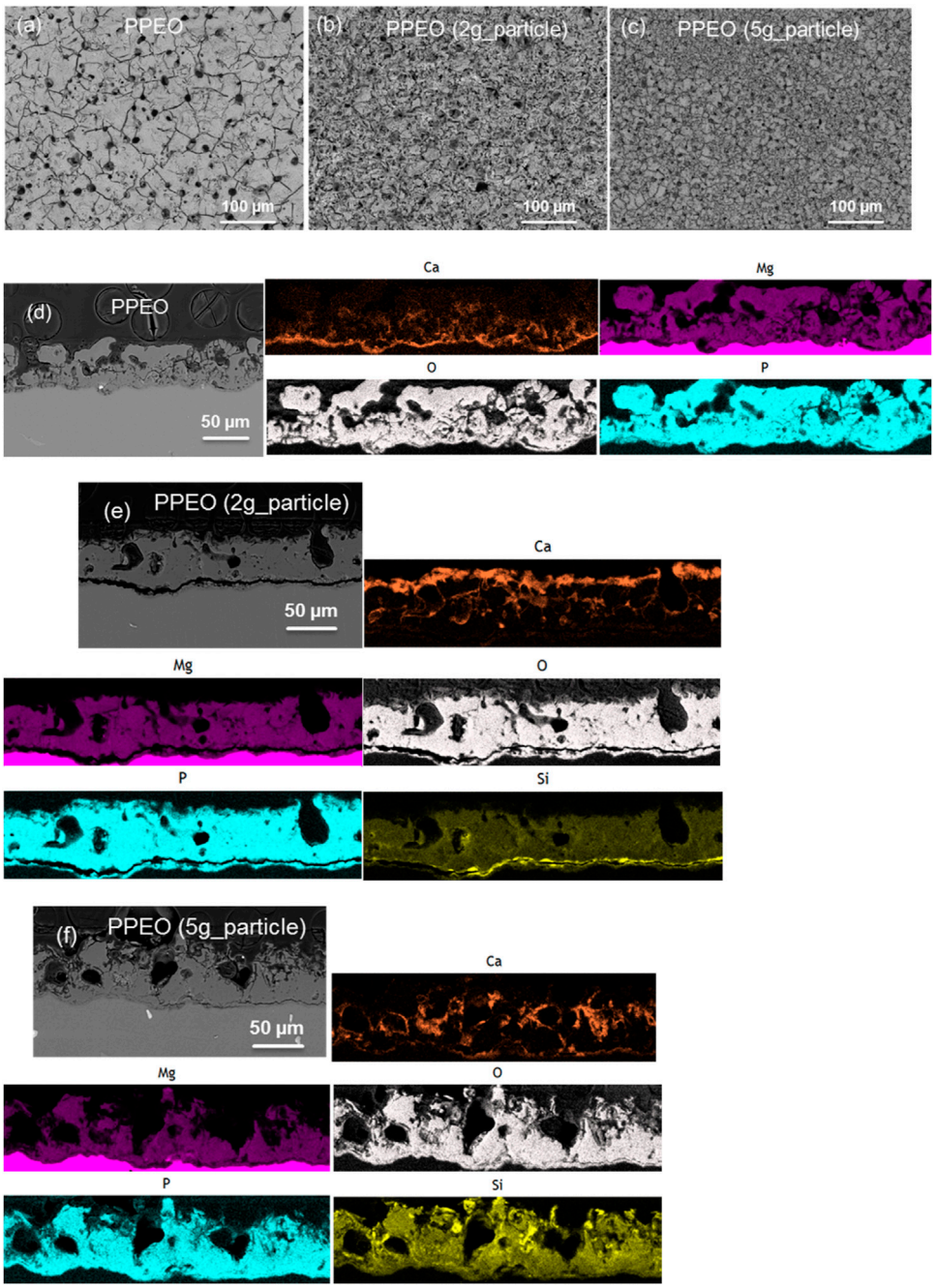

FIGURE 3 | Surface and cross section morphology of the PEO coatings after 3-days corrosion test. **(A)** and **(D)** PPEO, **(B)** and **(E)** PPEO (2 g_particle), **(C)** and **(F)** PPEO (5 g_particle).

layer seems to be peeled off from the matrix after preparation process, suggesting that the coating is severely corroded after immersion test. However, the surface porosity of the coating in the presence of particles is much less than the blank coating. Based on the EDS results (**Table 1**), it can be observed that the content of P and Na is reduced after performing corrosion test, while the content of Si and Al exhibits some kind of increase when compared to the uncorroded specimens. Ca is identified in all coatings, indicating that corrosion products are deposited on the coating surface by absorbing the soluble Ca^{2+} ions from the corrosive medium. Coating formed in the electrolyte containing 2 g/L nanoparticles has absorbed higher amount of Ca (5%) in contrast to the other two coatings, 0.5% for PPEO and 2.5% for PPEO (5 g_particle), respectively.

EDS maps were further performed to identify the element distribution of the corroded coatings after immersion for 3 days.

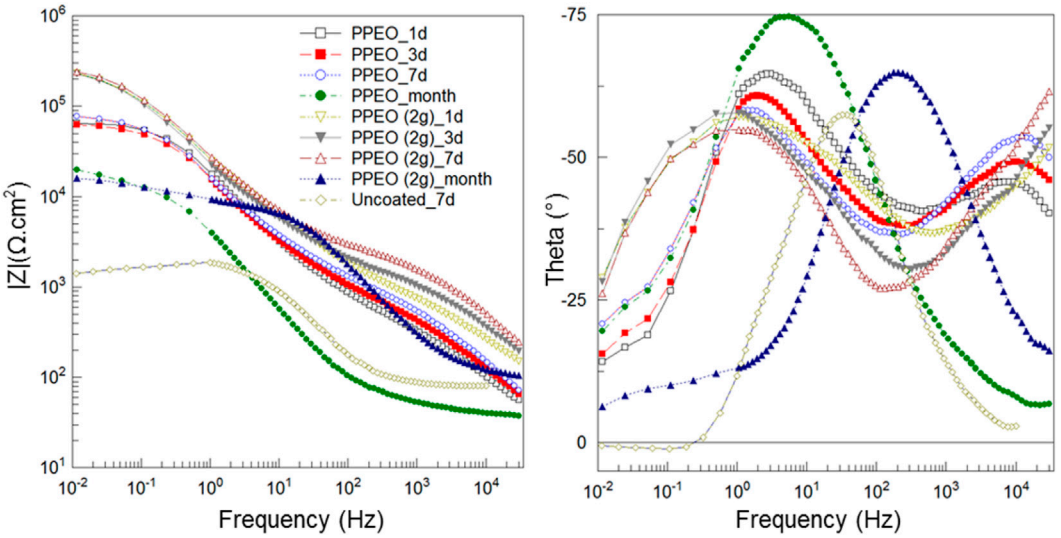

FIGURE 4 | Electrochemical impedance performance of PPEO and PPEO (2 g_particle) in Hank's solution.

For PPEO (**Figure 3D**), Ca is mainly enriched in the area between the outer and inner layer, namely the pore band, indicating that the corrosive medium has penetrated through the whole layer and reached the coating/matrix interface. A new layer (**Figure 3E**) composed of Ca, P, and O is clearly seen on the top of the primary outer layer for coating with addition of 2 g/L nanoparticles. In addition, some internal defects are sealed by the deposited corrosion products. As for the coating produced from electrolyte containing 5 g/L particles (**Figure 3F**), Ca signal is detected in the outer layer and also the inner part of the coating. Plenty of large-sized defects/cracks are observable in the layer, indicating that the dissolution rate of the original coating is faster than redeposition rate of the corrosion products formed by the components of the coating and corrosive electrolyte. Therefore, this type of coating is not applicable for acting as biodegradable layer for Mg alloy. According to the above-mentioned findings, it can be inferred that the amount and distribution of Ca element could be one criterion to judge the corrosion and self-repair degree of the coating. The crystallinity of the outer layer is also of great importance since it serves as primary protective barrier, and the redeposited corrosion layer acts as the secondary barrier layer for the matrix.

Electrochemical impedance spectroscopy (EIS) was employed to investigate the degradation behavior of the PEO coatings in Hank's solution, as can be seen in **Figure 4**. The high frequency time constant, corresponding to the outer layer of PEO coating, has been maintained for the first 1 week. It disappears after 1-month corrosion test, suggesting that the protective capability of the outer layer is strongly weakened. Taking the corroded coating microstructure into consideration, the maintenance of the time constant at high frequency suggests that the outer porous layer is sealed by the redeposited conversion products, and the merged time constants at the medium and low frequency could be associated to the inner layer and corrosion process respectively. This is an indication that the coating is corrosion resistant at the initial stage and is degradable after relatively long-term immersion test.

Additionally, the cytotoxicity of the coatings without and with addition of 2 g/L nanoparticles was evaluated by live/dead staining coupled with the SEM observation (**Figure 5**). The cytotoxicity of the uncoated sample was also investigated to compare with the coatings. As expected, cells cannot survive on the uncoated Mg without coating protection. The beneficial effect of PPEO coating on cell viability can be seen clearly and human osteoblasts were able to grow all over the surface. Furthermore, the cells appeared healthy, well-spread and possessed flattened morphology. Such phenotype is required for proper proliferation of anchorage-dependent cells (Walker et al., 2005). However, the results obtained from particle-containing coating are somehow unexpected, as only few cells were found after 7 days. The lower cell density could be explained by the rapid degradation of the coating rather than toxicity of the coating itself as flower-like corrosion products were observed on the coating surface. The discrepancy between degradation behaviors in various *in vitro* tests can be mainly attributed to the different total amount of the Ca^{2+} ions in the corrosion medium used for testing. The volume of Hank's solution (330 ml) for electrochemical measurements is much higher than that of DMEM solution (6 ml) used for cytotoxicity test, although the concentration of Ca^{2+} ions of each medium is comparable. There is a high probability of depletion of Ca^{2+} in the DMEM electrolyte which leads to unrealistically low concentrations of this cation after certain time. As it is demonstrated above, Ca^{2+} ions play a crucial role in the controllable degradation of PEO coated Mg alloy. Consequently, the reduced concentration of Ca^{2+} in the testing media could suppress the self-healing ability of the developed coatings. Moreover, cytotoxicity test was performed under physiological conditions, e.g., cell culture media, 37°C, 5% CO_2, and presence of proteins, which are known to influence the corrosion rate of the coating (Willumeit et al., 2013).

Summarizing, introduction of SiO_2 nanoparticles to the electrolyte results in PEO coatings with different microstructure and phase composition, as the crystalline coating turns into

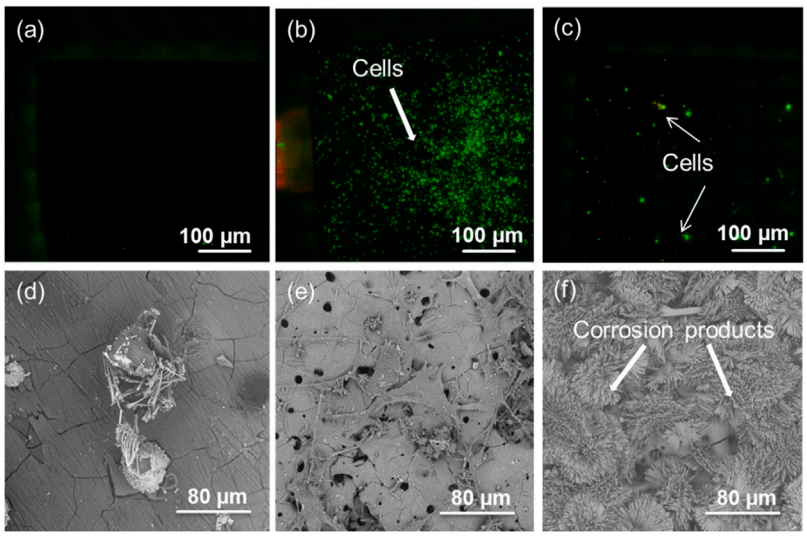

FIGURE 5 | Live/dead staining and SEM observation on the surface of uncoated and coated Mg alloy after cell culture for 7 days. **(A)** and **(D)** uncoated Mg, **(B)** and **(E)** PPEO, **(C)** and **(F)** PPEO (2 g_particle).

amorphous layer due to the reactively incorporated nanoparticles, which have huge effects on the corrosion response and degradation behavior. It can be inferred that the degradation process of the coating is also influenced by the place of implantation, which determines the volume, flow velocity and chemical composition of the surrounding corrosive medium, leading to huge discrepancies when using different *in vitro* testing methods. Principally the corrosion mechanism and degradation process of the coating can be summarized as follows. Due to dissolution of unstable amorphous material, reprecipitation of low-solubility compounds initiates when the corrosive surroundings provide appropriate ions. For example, Ca^{2+} ions from the body fluid/blood can react with the dissolved phosphate, silicate or hydroxide ions from the dissolved layer and redeposit on the coating surface. Meanwhile, the pore band between the outer and inner layer can be considered as a reservoir for the newly formed conversion products, most likely to be calcium compounds. In that sense, the porosity of PEO coating can be taken as advantage to significantly improve the bonding area with the corrosive medium to form a new protective bioactive layer. It is noteworthy that the designed coatings are only capable of delaying the degradation of Mg alloy at the initial stage rather than the later stage, which is of paramount importance for biomedical application. The degradation process of the coating in flowing surrounding should be investigated in future work.

4 CONCLUSION

The degradation rate of PEO coating in simulated body fluid could be controlled by varying the coating composition, which is mainly balanced by dissolution of the unstable amorphous material and reconstruction of the redeposited conversion products. The crystallinity of the outer layer is of great importance since it serves as primary protective barrier, while the redeposited corrosion layer acts as the secondary barrier layer, which is primarily related to the degree of amorphization of the coating. The self-healing capability enables PEO process to be an applicable surface treatment approach for Mg based implant materials. With these findings it is possible to design PEO coatings with certain degradation rate for biomedical application.

DATA AVAILABILITY STATEMENT

The original contributions presented in the study are included in the article/Supplementary Material, further inquiries can be directed to the corresponding author.

AUTHOR CONTRIBUTIONS

XL, CB, BL, and MZ contributed to conception and design of the study. XL and BL performed the statistical analysis. XL wrote the first draft of the manuscript. CB, BL, and MZ wrote sections of the manuscript. All authors contributed to manuscript revision, read, and approved the submitted version.

ACKNOWLEDGMENTS

The technical support of V. Heitmann and U. Burmester is gratefully acknowledged. The authors would like to acknowledge the financial support from National Natural Science Foundation of China (No. 52071067), Mobility Programme of the Sino-German Center (M-0056) and Fundamental Research Funds for the Central Universities (N2002009).

REFERENCES

Arrabal, R., Matykina, E., Hashimoto, T., Skeldon, P., and Thompson, G. E. (2009). Characterization of AC PEO Coatings on Magnesium Alloys. *Surf. Coat. Technology* 203, 2207–2220. doi:10.1016/j.surfcoat.2009.02.011

Blawert, C., Sah, S. P., Scharnagl, N., and Kannan, M. B. (2015). "Plasma Electrolytic Oxidation/micro-Arc Oxidation of Magnesium and its Alloys," in *Surface Modification of Magnesium and its Alloys for Biomedical Applications*. Editors Narayanan, T. S. N. S., and Lee, I.-S. P.-H. (Woodhead Publishing), 193–234. doi:10.1016/b978-1-78242-078-1.00008-6

Cha, P. R., Han, H. S., Yang, G. F., Kim, Y. C., Hong, K. H., Lee, S. C., et al. (2013). Biodegradability Engineering of Biodegradable Mg Alloys: Tailoring the Electrochemical Properties and Microstructure of Constituent Phases. *Sci. Rep.* 3, 2367. doi:10.1038/srep02367

Córdoba, L. C., Montemor, M. F., and Coradin, T. (2016). Silane/TiO2 Coating to Control the Corrosion Rate of Magnesium Alloys in Simulated Body Fluid. *Corrosion Sci.* 104, 152–161.

Gnedenkov, A. S., Sinebryukhov, S. L., Mashtalyar, D. V., and Gnedenkov, S. V. (2016). Protective Properties of Inhibitor-Containing Composite Coatings on a Mg alloy. *Corrosion Sci.* 102, 348–354. doi:10.1016/j.corsci.2015.10.026

Gu, X. N., Li, N., Zhou, W. R., Zheng, Y. F., Zhao, X., Cai, Q. Z., et al. (2011). Corrosion Resistance and Surface Biocompatibility of a Microarc Oxidation Coating on a Mg-Ca alloy. *Acta Biomater.* 7, 1880–1889. doi:10.1016/j.actbio.2010.11.034

Hort, N., Huang, Y., Fechner, D., Störmer, M., Blawert, C., Witte, F., et al. (2010). Magnesium Alloys as Implant Materials - Principles of Property Design for Mg-RE Alloys☆. *Acta Biomater.* 6, 1714–1725. doi:10.1016/j.actbio.2009.09.010

Hu, R.-G., Zhang, S., Bu, J.-F., Lin, C.-J., and Song, G.-L. (2012). Recent Progress in Corrosion protection of Magnesium Alloys by Organic Coatings. *Prog. Org. Coat.* 73, 129–141. doi:10.1016/j.porgcoat.2011.10.011

Ke, C., Wu, Y., Qiu, Y., Duan, J., Birbilis, N., and Chen, X.-B. (2016). Influence of Surface Chemistry on the Formation of Crystalline Hydroxide Coatings on Mg Alloys in Liquid Water and Steam Systems. *Corrosion Sci.* 113, 145–159. doi:10.1016/j.corsci.2016.10.017

Kirkland, N. T., Lespagnol, J., Birbilis, N., and Staiger, M. P. (2010). A Survey of Bio-Corrosion Rates of Magnesium Alloys. *Corrosion Sci.* 52, 287–291. doi:10.1016/j.corsci.2009.09.033

Lu, X., Blawert, C., Zheludkevich, M. L., and Kainer, K. U. (2015). Insights into Plasma Electrolytic Oxidation Treatment with Particle Addition. *Corrosion Sci.* 101, 201–207. doi:10.1016/j.corsci.2015.09.016

Mei, D., Lamaka, S. V., Lu, X., and Zheludkevich, M. L. (2020). Selecting Medium for Corrosion Testing of Bioabsorbable Magnesium and Other Metals - A Critical Review. *Corrosion Sci.* 171, 108722. doi:10.1016/j.corsci.2020.108722

Mei, D., Wang, C., Lamaka, S. V., and Zheludkevich, M. L. (2021). Clarifying the Influence of Albumin on the Initial Stages of Magnesium Corrosion in Hank's Balanced Salt Solution. *J. Magnesium Alloys* 9, 805–817.

Miskovic, D. M., Pohl, K., Birbilis, N., Laws, K. J., and Ferry, M. (2017). Formation of a Phosphate Conversion Coating on Bioresorbable Mg-Based Metallic Glasses and its Effect on Corrosion Performance. *Corrosion Sci.* 129, 214–225. doi:10.1016/j.corsci.2017.10.014

Mori, Y., Koshi, A., Liao, J., Asoh, H., and Ono, S. (2014). Characteristics and Corrosion Resistance of Plasma Electrolytic Oxidation Coatings on AZ31B Mg alloy Formed in Phosphate - Silicate Mixture Electrolytes. *Corrosion Sci.* 88, 254–262. doi:10.1016/j.corsci.2014.07.038

Sankara Narayanan, T. S. N., Park, I. S., and Lee, M. H. (2014). Strategies to Improve the Corrosion Resistance of Microarc Oxidation (MAO) Coated Magnesium Alloys for Degradable Implants: Prospects and Challenges. *Prog. Mater. Sci.* 60, 1–71. doi:10.1016/j.pmatsci.2013.08.002

Shi, P., Ng, W. F., Wong, M. H., and Cheng, F. T. (2009). Improvement of Corrosion Resistance of Pure Magnesium in Hanks' Solution by Microarc Oxidation with Sol-Gel TiO2 Sealing. *J. Alloys Compounds* 469, 286–292. doi:10.1016/j.jallcom.2008.01.102

Song, J., She, J., Chen, D., and Pan, F. (2020). Latest Research Advances on Magnesium and Magnesium Alloys Worldwide. *J. Magnesium Alloys* 8, 1–41. doi:10.1016/j.jma.2020.02.003

Song, Y. W., Shan, D. Y., and Han, E. H. (2007). Corrosion Behaviors of Electroless Plating Ni-P Coatings Deposited on Magnesium Alloys in Artificial Sweat Solution. *Electrochimica Acta* 53, 2009–2015. doi:10.1016/j.electacta.2007.08.062

Staiger, M. P., Pietak, A. M., Huadmai, J., and Dias, G. (2006). Magnesium and its Alloys as Orthopedic Biomaterials: A Review. *Biomaterials* 27, 1728–1734. doi:10.1016/j.biomaterials.2005.10.003

Sun, M., Yerokhin, A., Bychkova, M. Y., Shtansky, D. V., Levashov, E. A., and Matthews, A. (2016). Self-healing Plasma Electrolytic Oxidation Coatings Doped with Benzotriazole Loaded Halloysite Nanotubes on AM50 Magnesium alloy. *Corrosion Sci.* 111, 753–769. doi:10.1016/j.corsci.2016.06.016

Tie, D., Guan, R., Liu, H., Chen, M., Ulasevich, S. A., Skorb, E. V., et al. (2021). *In Vivo* degradability and Biocompatibility of a Rheo-Formed Mg–Zn–Sr alloy for Ureteral Implantation. *J. Magnesium Alloys*. 7:254–262.

Walker, J. L., Fournier, A. K., and Assoian, R. K. (2005). Regulation of Growth Factor Signaling and Cell Cycle Progression by Cell Adhesion and Adhesion-dependent Changes in Cellular Tension. *Cytokine Growth Factor. Rev.* 16, 395–405. doi:10.1016/j.cytogfr.2005.03.003

Willumeit, R., Feyerabend, F., and Huber, N. (2013). Magnesium Degradation as Determined by Artificial Neural Networks. *Acta Biomater.* 9, 8722–8729. doi:10.1016/j.actbio.2013.02.042

Wu, G., Ibrahim, J. M., and Chu, P. K. (2013). Surface Design of Biodegradable Magnesium Alloys - A Review. *Surf. Coat. Technology* 233, 2–12. doi:10.1016/j.surfcoat.2012.10.009

Yang, L., He, S., Yang, C., Zhou, X., Lu, X., Huang, Y., et al. (2021). Mechanism of Mn on Inhibiting Fe-Caused Magnesium Corrosion. *J. Magnesium Alloys* 9, 676–685. doi:10.1016/j.jma.2020.09.015

Zhang, L., Zhang, J., Chen, C.-f., and Gu, Y. (2015). Advances in Microarc Oxidation Coated AZ31 Mg Alloys for Biomedical Applications. *Corrosion Sci.* 91, 7–28. doi:10.1016/j.corsci.2014.11.001

Zhang, Y., Feyerabend, F., Tang, S., Hu, J., Lu, X., Blawert, C., et al. (2017). A Study of Degradation Resistance and Cytocompatibility of Super-hydrophobic Coating on Magnesium. *Mater. Sci. Eng. C* 78, 405–412. doi:10.1016/j.msec.2017.04.057

Conflict of Interest: The authors declare that the research was conducted in the absence of any commercial or financial relationships that could be construed as a potential conflict of interest.